Materials Science & Engineering C 120 (2021) 111757

Contents lists available at ScienceDirect

Materials Science & Engineering C

journal homepage: www.elsevier.com/locate/msec

Green fabrication of Cu/rGO decorated SWCNT buckypaper as a flexible electrode for glucose detection

Tianxiang Zhu [a,b], Xiaoer Wang [a,b], Weiwei Chang [a,b], Yifan Zhang [a,b], Takahiro Maruyama [c], Liqiang Luo [d,*], Xinluo Zhao [a,b,**]

[a] Department of Physics, Shanghai University, Shanghai 200444, China
[b] Institute of Low-dimensional Carbons and Device Physics, Shanghai University, Shanghai 200444, China
[c] Department of Applied Chemistry, Meijo University, Nagoya 468-8502, Japan
[d] Department of Chemistry, Shanghai University, Shanghai 200444, China

ARTICLE INFO

Keywords:
Buckypaper
Single-walled carbon nanotube
Graphene oxide
Flexible electrode
Electrochemical biosensor

ABSTRACT

As a paper-like membrane composed of single-walled carbon nanotube (SWCNT), buckypaper possesses high conductivity, ideal flexibility, large surface area, great thermal/chemical stability and biocompatibility, which has manifested its potential as an alternative support material. However, due to the lack of defects, high quality SWCNT synthesized by arc-discharge method is difficult to be modified with metal nanoparticles for electro-catalysis. In this paper, a novel green strategy has been developed to fabricate SWCNT buckypaper decorated with Cu/reduced graphene oxide (Cu/rGO-BP) for the first time, in which graphene oxide functions as the intermediate between SWCNT and Cu nanoparticles. The fabricated Cu/rGO-BP was applied as a flexible electrode for electrochemical glucose detection. The electrode exhibited excellent electro-catalytic activity for glucose oxidation. The sensor based on Cu/rGO-BP performed a high upper limit of linear range (25 mM), which is close to commercial glucose sensors. The proposed strategy for Cu/rGO-BP fabrication can be extended to modify buckypaper with other metal or metal oxide nanoparticles, and thus opens an innovative route to potential practical applications of flexible buckypaper in wearable bioelectronics.

1. Introduction

Carbon nanotubes have attracted increasing attention from both academic and industrial communities for its outstanding properties [1–3]. Buckypaper, a paper-like membrane composed of carbon nanotubes, has been applied as a novel support material for biofuel cells [4], strain sensors [5], supercapacitors [6] and cell transplantation [7]. Among different kinds of carbon nanotubes, single-walled carbon nanotube (SWCNT) synthesized by arc-discharge method exhibits ideal chemical stability as well as excellent mechanical, thermal and electrical properties [8]. Therefore, the buckypaper composed of arc-discharge SWCNT is a promising material for flexible electronics. However, due to the lack of defects and functional groups on its surface, arc-discharge SWCNT is difficult to be modified with metal or metal oxide nanoparticles, which extremely limits its application in electro-catalysis. To our knowledge, few reports focus on flexible buckypaper consisting of catalyst-modified SWCNT as a substitute of rigid electrodes for electro-catalysis. Recently, our group has developed flexible SWCNT buckypaper for electrochemical determination of glucose, in which Ni/SWCNT nanocomposites were in situ synthesized via arc-discharge method [9]. Nevertheless, only a few kinds of functional nanoparticles can be loaded on SWCNT with this method, and new approaches become highly desirable for the fabrication of flexible and wearable electrochemical devices.

In contrast with arc-discharge SWCNT, graphene oxide (GO) is soluble in common solvents and much easier to be modified, which is attributed to the abundant functional groups on its surface [10]. For example, Dezfuli et al. anchored Sm_2O_3 onto reduced graphene oxide (rGO) via a sonochemical procedure for supercapacitors [11]. Atchudan et al. synthesized ZnO/GO composite through solvothermal route for methylene blue degradation [12]. Wu et al. modified GO with chitosan by CO_2 supercritical drying for bilirubin removal [13].

Diabetes is one of the most frequent chronic diseases that risk human health, and the world's diabetic population has been predicted to keep

* Corresponding author.
** Correspondence to: X. Zhao, Department of Physics, Shanghai University, Shanghai 200444, China.
E-mail addresses: luck@shu.edu.cn (L. Luo), xlzhao@shu.edu.cn (X. Zhao).

https://doi.org/10.1016/j.msec.2020.111757
Received 30 April 2020; Received in revised form 27 October 2020; Accepted 21 November 2020
Available online 27 November 2020

growing by 2030 [14]. For the patients, daily glucose monitoring is vital to ensure that they can receive proper healthcare. Thus, wearable glucose sensor is a promising direction of novel biosensors, and flexible electrodes with catalytic activity for glucose oxidation play a significant role in wearable electrochemical glucose sensors.

Cu and its oxides (CuO and Cu_2O) have attracted a lot of interests in electrochemical glucose sensors on account of their cheapness, non-toxicity and chemical stability [15,16]. For instance, Yang et al. adjusted the valence state of ZIF-67 with Cu_2O for glucose detection [17]; Wu el al. reported a glucose sensor based on multi-walled carbon nanotube (MWCNT) modified by Cu-based metal-organic framework (MOF), which exhibited ultra-high sensitivity [18]; Sun et al. fabricated porous CuO/carbon cloth composites through a hydrothermal method for glucose sensing [19].

In this work, we report an environment-friendly and low-cost strategy to fabricate Cu/rGO decorated SWCNT buckypaper (Cu/rGO-BP). GO was introduced as the intermediate between Cu nanoparticles and SWCNT buckypaper. The precursor, $Cu(OH)_2$, was anchored on GO via a solution process. To obtain Cu/rGO-BP, GO and $Cu(OH)_2$ were simultaneously reduced during a thermal treatment in H_2 after they had been vacuum filtrated on the SWCNT buckypaper. Especially, rGO can be well fixed on SWCNT without any binder due to their similar sp^2 structure. As a concept of biosensor application, Cu/rGO-BP was assessed as a flexible electrode for electrochemical glucose detection. It was found that the upper limit of the sensor's linear range could reach 25 mM. The result reveals that the nanocomposites fabricated through this novel strategy can take advantage of SWCNT buckypaper with ideal flexibility and conductivity, as well as Cu nanoparticles with high catalytic activity. Additionally, the strategy is extensible, which can be applied to the fabrication of buckypaper modified with other functional nanoparticles, such as Ag, Pd, Pt, Au, Al_2O_3, TiO_2, MnO_2 and ZnO. All in all, the developed strategy puts forward an alternative way to extend the potential practical applications of buckypaper in flexible and wearable biosensors.

2. Experimental section

2.1. Chemicals

GO (dispersed in water, size: >500 nm) was purchased from Nanjing XFNANO Materials Tech Co., Ltd., China. Glucose, dopamine hydrochloride and $Cu(CH_3COO)_2$ were received from Sigma-Aldrich, USA. Human blood serum samples were offered by Longhua Hospital Affiliated to Shanghai University of Traditional Chinese Medicine. Other chemicals were bought from Sinopharm Group Co., Ltd., China.

2.2. Instrumental

The samples were characterized by scanning electron microscopy (SEM, Hitachi SU5000, Japan), element energy dispersive spectroscopy (EDS, EDAX E1367-C2B, USA), X-ray diffraction (XRD, Rigaku D/MAX-2200, Japan, power: 3 kW) with Cu Kα radiation, X-ray photoelectron spectroscopy (XPS, ESCALAB 250Xi, UK) using Al Kα radiation, transmission electron microscopy (TEM, JEOL JEM-2100F, Japan, accelerating voltage: 200 kV), Raman spectroscopy (Renishaw InVia, UK) with 532 nm laser excitation (laser power: 3 mW) and 4-probe resistivity measurement system (Probes Tech RTS-8, China).

2.3. Fabrication of Cu/rGO-BP

SWCNT was prepared by a Fe-catalyzed arc-discharge method in H_2/He atmosphere [20] and purified using the method reported by our group before [21]. The purified SWCNT was added into deionized water after being crushed, and the SWCNT/water mixture was vacuum filtrated to form SWCNT buckypaper.

The precursor, $Cu(OH)_2$, was decorated on GO via a solution method [22]. Briefly, GO was mixed with $Cu(CH_3COO)_2$ in deionized water under stirring for 30 min. Afterwards, excessive NaOH was added into the dispersion of GO/$Cu(CH_3COO)_2$ to get $Cu(OH)_2$/GO.

To obtain Cu/rGO-BP, $Cu(OH)_2$/GO was vacuum filtrated onto the SWCNT layer, followed by thermal treatment in flowing H_2/Ar at 450–550 °C (step: 50 °C) for 30 min.

2.4. Electrochemical measurements

The electrochemical properties of the fabricated Cu/rGO-BP were measured by an electrochemical workstation (Chenhua CHI-660C, China) at room temperature. All measurements were based on a traditional three-electrode system: Pt foil, Hg/HgO electrode (1 M KOH) and Cu/rGO-BP corresponded to the counter, reference and working electrodes, respectively. Current-time (I-t) curve was recorded while glucose aqueous solution was successively added into the electrolyte under stirring.

3. Results and discussion

3.1. Design and fabrication strategy of Cu/rGO-BP

To design Cu-modified flexible electrodes, two kinds of low-dimensional carbon materials (LCMs) with different properties have been utilized: SWCNT and GO. As illustrated in Scheme 1, each step of the fabrication strategy is green and facile without any toxic or strong oxidizing chemicals. 500 °C was found the most suitable temperature for the thermal treatment to produce Cu/rGO composite: $Cu(OH)_2$ was not completely reduced at 450 °C, while GO would be severely consumed by H_2 at 550 °C. Therefore, the following experiements were performed based on 500 °C-treated samples. The fabricated Cu/rGO-BP has a double-layer structure: the conductive support layer of SWCNT and the catalyst layer of Cu/rGO. As shown in Fig. 1a, a coin-sized piece of Cu/rGO-BP could recover to its original shape after it had been folded in half twice, indicating the great flexibility of buckypaper. For electrochemical tests, small pieces of buckypaper were cut from large pieces. In our laboratory, the available maximal size of buckypaper can be 4 cm in diameter, whereas each piece used as the working electrode is only 4 × 4 mm^2. Technically, by simply extending the size of the filter and heating chamber, it is possible to prepare larger Cu/rGO-BP.

Furthermore, this strategy is widely applicable. With proper precursors for metal or metal oxide, the strategy can be applied to buckypaper decorated with different catalysts: For reactive metals that cannot be produced by H_2 reduction, the final product should be metal oxide nanoparticles (Al_2O_3, TiO_2, MnO_2, ZnO, etc.); For inert metals, the final product should be metal nanoparticles (Ag, Pd, Pt, Au, etc.). Actually, ZnO/rGO-decorated SWCNT buckypaper has been successfully fabricated in our laboratory through this method.

3.2. Morphological characterization

As displayed in Fig. 1b, GO was covered with amorphous $Cu(OH)_2$ after the solution process. The morphology of the SWCNT layer in Cu/rGO-BP is shown in Fig. 1c. Obviously, the fibers are SWCNT bundles. Since the diameter of an individual SWCNT is about 1 nm, each bundle is composed of multiple SWCNTs. Besides, no impurities are visible, indicating that both amorphous carbon and metal catalyst in as-grown SWCNT was removed during the purification process. Herein, highly purified SWCNT can ensure the ideal mechanical and electrical properties of the support layer. Fig. 1d shows the typical SEM image of the Cu/rGO layer. Cu nanoparticles, whose diameters range from 100 to 150 nm, are densely loaded on rGO sheets. Moreover, rGO keeps its 2D structure after the reduction process. EDS analysis (Fig. S1) for a 40 × 40 μm^2 region in the Cu/rGO layer is listed in Table 1. The mass percentage of Cu is 70.26%. The Cu/rGO ratio is controllable by adjusting the amount of GO and $Cu(CH_3COO)_2$ used in the solution process.

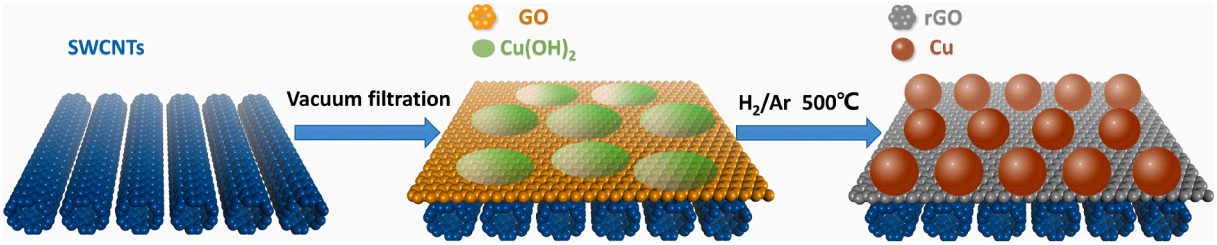

Scheme 1. Schematic illustration of the fabrication strategy for Cu/rGO-BP.

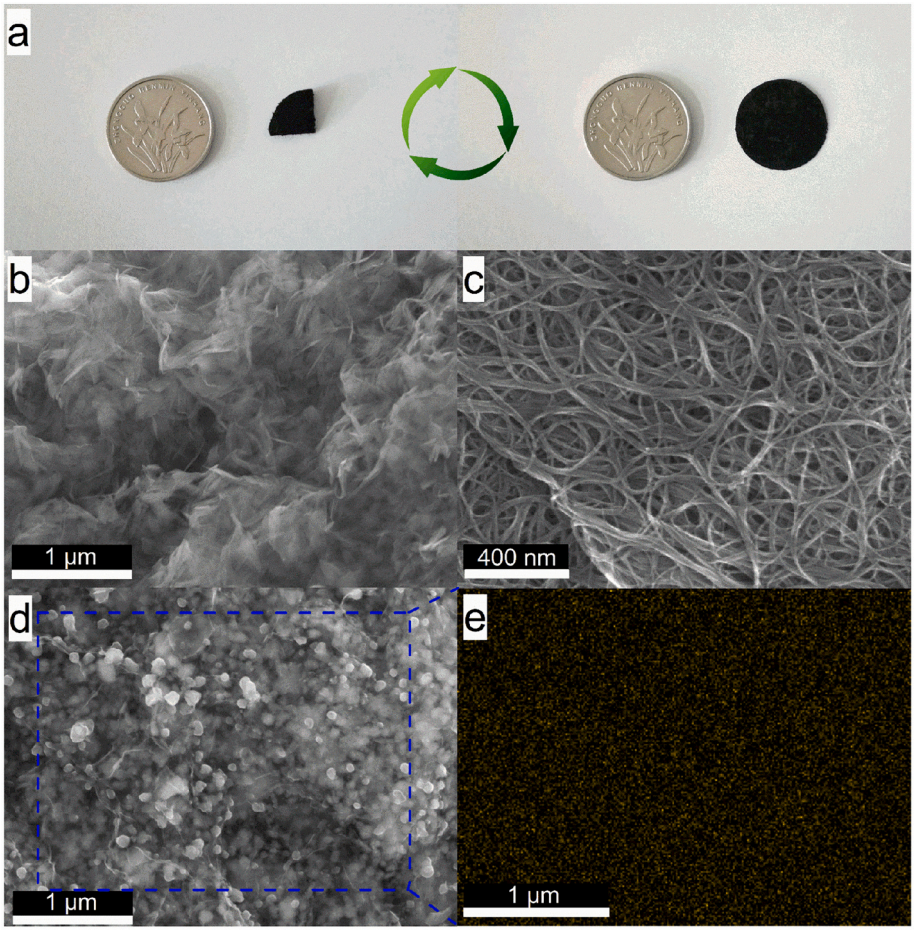

Fig. 1. (a) Photographs of Cu/rGO-BP. SEM images of (b) $Cu(OH)_2$-coated GO, (c) the SWCNT layer and (d) the Cu/rGO layer of Cu/rGO-BP. (e) EDS mapping of Cu in the Cu/rGO layer.

Table 1
EDS analysis of Cu/rGO-BP.

Element	Weight %	Atomic %
C K	12.27	34.75
O K	11.48	24.41
Cu K	76.26	40.84

Besides, the detected oxygen might be from the residual oxygen-containing functional groups in rGO and O_2 absorbed on the surface of buckypaper. According to the EDS mapping (Fig. 1e) of the selected area in Fig. 1d, Cu nanoparticles have been uniformly distributed in Cu/rGO-BP.

3.3. Structural characterization

XRD was employed to check the reduction effect of the thermal treatment in H_2. The peak positions of Cu and graphite are based on JCPDS cards. Fig. 2 shows the XRD patterns of GO and Cu/rGO. For GO, the peak at 10.6° corresponds to the typical interlayer distance of GO, while the broad peak at about 21.5° is from the less-oxidized sp^2 domains in GO [23]. Compared to the (002) peak of graphite at 26.5°, the (002) peak of GO shifts to lower degree, indicating that even sp^2 domains in GO have larger interlayer distance than graphite. For Cu/rGO, the peak at 10.6° totally disappears and the (002) peak shifts to 25.3°, indicating that the inter-layer distance of rGO is much closer to that of graphite due to the removal of oxygen-containing groups in GO. Additionally, the (111) and (200) peaks from Cu are observed at 43.1° and 50.3°, respectively. On the other hand, no peaks from Cu oxides are identifiable. The XRD analysis reveals that the reduction method can

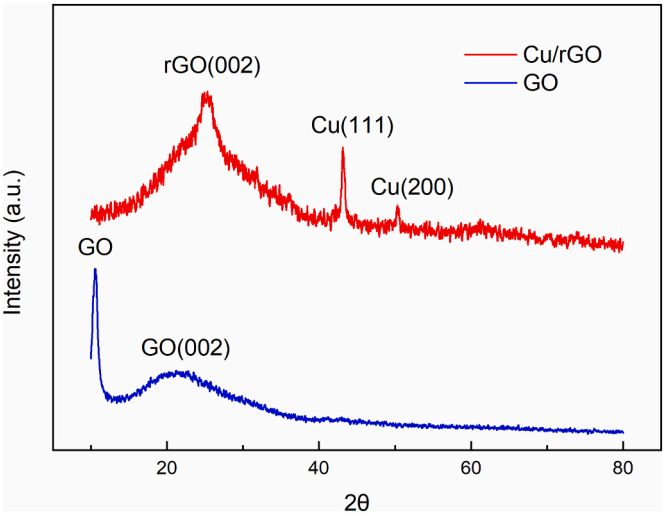

Fig. 2. XRD patterns of GO and Cu/rGO.

efficiently reduce $Cu(OH)_2$/GO into Cu/rGO. Furthermore, GO and Cu/rGO were characterized by XPS (Fig. S2), which confirmed the removal of oxygen-containing groups in GO.

TEM image of Cu nanoparticles loaded on rGO is presented in Fig. 3a. From the high- resolution TEM (HRTEM) image of a Cu nanoparticle, the lattice spacing measured from this image is 0.21 nm, corresponding to the (111) planes of Cu. Furthermore, selected area electron diffraction (SAED) for Cu nanoparticles on rGO was conducted. From the SAED patterns in Fig. 3b, diffraction rings of Cu(111) and (200) can be observed. In a word, the HRTEM and SAED results are consistent with the XRD analysis.

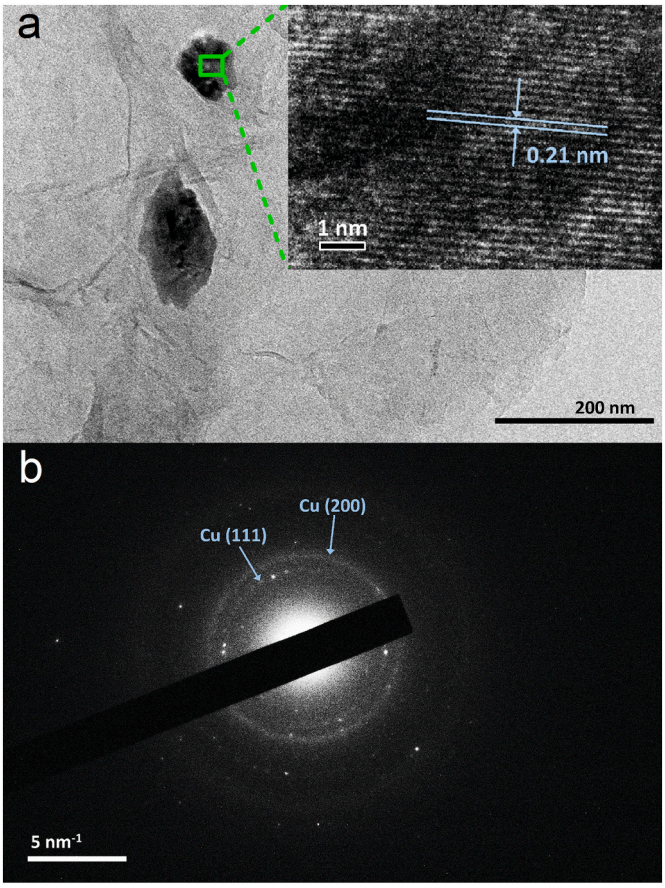

Fig. 3. (a) TEM image of Cu/rGO (inset: HRTEM image of a Cu nanoparticle). (b) SAED patterns of Cu nanoparticles.

Raman spectra of SWCNT, GO and Cu/rGO were recorded for further analysis of their structures. There are three distinct bands in the SWCNT spectrum displayed in Fig. 4a [24]:G band at 1588 cm^{-1} is originated from the in-plane vibration of sp^2 carbon network, which is broadened by the peak at 1552 cm^{-1} because the sp^2 plane curls into a tube; D band at 1330 cm^{-1} is attributed to the defects in sp^2 carbon; the radial breathing mode peaks at 218, 227 and 264 cm^{-1} correspond to 1.13-, 1.08- and 0.92-nm-diameter SWCNTs, according to the following relation: $\omega_{RBM} = 234/d_t$ (nm) + 10 cm^{-1} [25]. The G/D band intensity ratio (I_G/I_D) is often calculated to evaluate the crystallinity of sp^2 carbon [26]. Herein, I_G/I_D for SWCNT is 34.2, indicating that it is less-defective. Therefore, high quality SWCNT helps to form the support layer of Cu/rGO-BP with good flexibility and conductivity. On the basis of Fig. 4b and c, I_G/I_D values for GO and rGO are 1.14 and 1.32, respectively. Moreover, the G band of rGO shifts from 1601 to 1587 cm^{-1} after the reduction process, which is in consensus with previous reports on rGO [27,28]. Combining XRD, XPS and Raman analysis, it can be inferred that the thermal treatment in H_2 at 500 °C can not only remove oxygen-containing groups in GO but also partially repair the defects in sp^2 domains.

3.4. Application of Cu/rGO-BP in glucose detection

The fabricated Cu/rGO-BP was applied as a flexible electrode for the electrochemical determination of glucose. The electro-catalytic activity of Cu/rGO-BP was evaluated by cyclic voltammetry (CV). In Fig. 5a, no oxidation peak is noticeable for bare SWCNT buckypaper in the presence or absence of 10 mM glucose. Actually, glucose should be oxidized at much higher potential on SWCNT, which is in great agreement with the literature [29]. For Cu/rGO-BP, however, a weak peak derived from Cu oxidation is visible at 0.4 V in the absence of glucose; while a much higher catalytic current peak appears at about the same potential in the presence of 10 mM glucose, indicating that glucose can be electro-

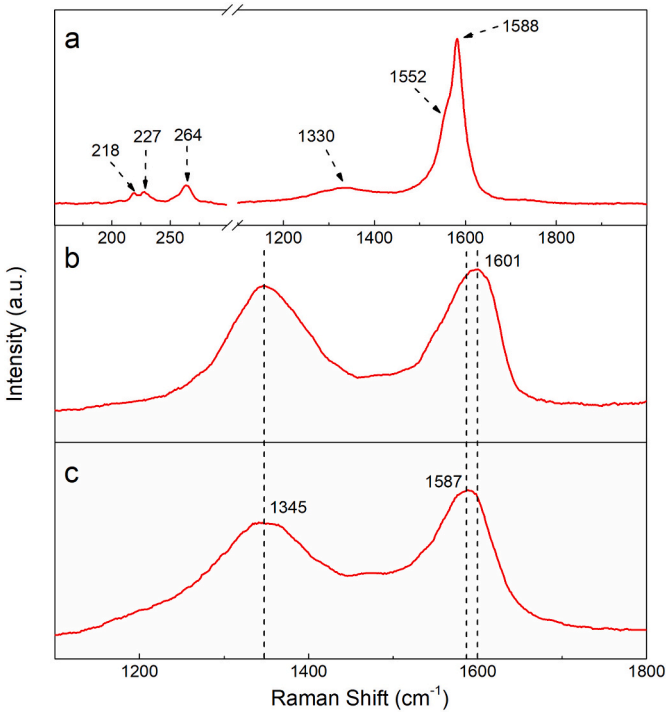

Fig. 4. Raman spectra of (a) SWCNT, (b) GO and (c) Cu/rGO (excitation wavelength: 532 nm).

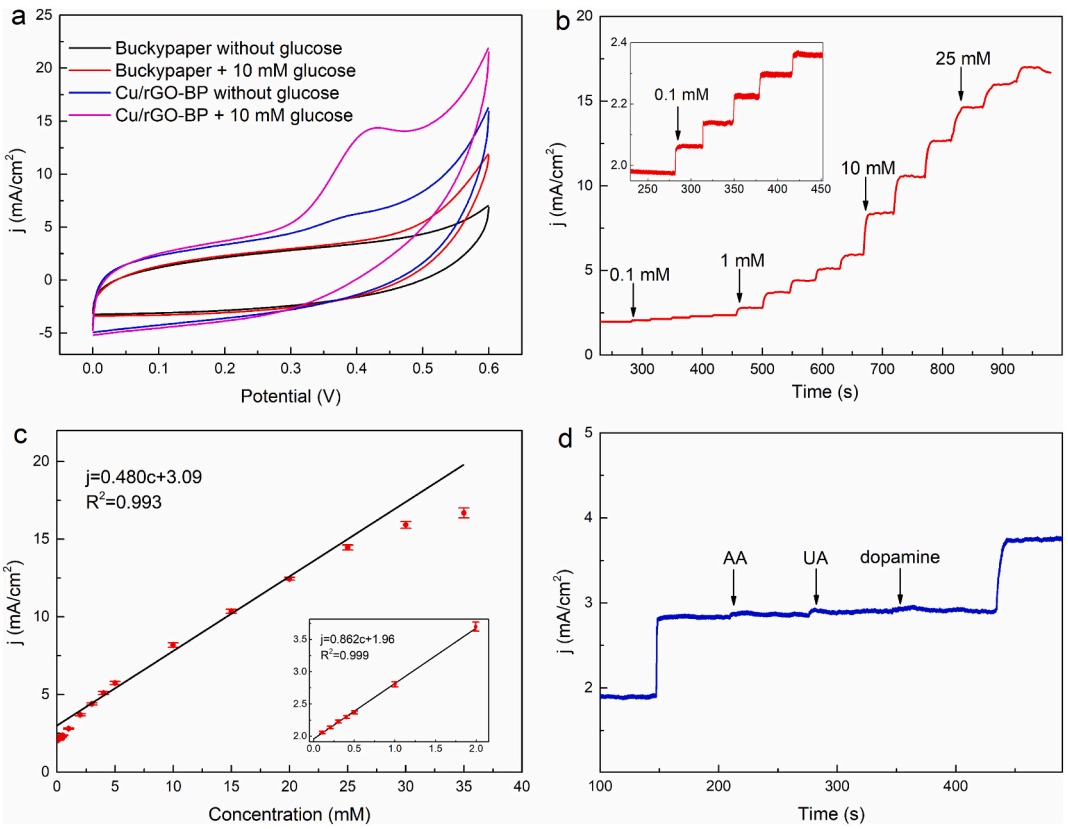

Fig. 5. (a) CVs of 10 mM glucose on bare buckypaper and Cu/rGO-BP in 0.4 M NaOH at scan rate of 20 mV/s. (b) Typical I-t curve of Cu/rGO-BP response to different concentrations of glucose at 0.4 V. (c) The corresponding plot of current density vs. glucose concentration. (d) Interference test for Cu/rGO-BP.

catalyzed with much lower overpotential due to the existence of Cu nanoparticles. CV investigations on the influences of NaOH concentration and scan rate were performed (Fig. S3). The results indicate that glucose oxidation reaction on Cu/rGO-BP was an adsorption-controlled process [30] and the oxidation peak position shifted from 0.48 to 0.4 V as NaOH concentration rose from 0.1 to 0.4 M, indicating better activity of the electrode in 0.4 M NaOH. According to the literature [31,32], the mechanism of glucose oxidation on Cu surface can be expressed as follows:

$$\mathrm{Cu} \xrightarrow{\text{alkaline}} \mathrm{Cu(II)} + 2e^- \quad (1)$$

$$\mathrm{Cu(II)} \xrightarrow{\text{alkaline, +0.4 V}} \mathrm{Cu(III)} + e^- \quad (2)$$

$$\mathrm{Cu(III)} + \text{glucose} \rightarrow \mathrm{Cu(II)} + \text{gluconic acid} \quad (3)$$

The amperometric response for glucose detection on Cu/rGO-BP is presented in Fig. 5b, and the corresponding current-concentration relation is plotted in Fig. 5c. Cu/rGO-BP exhibited two linear ranges for glucose detection: one was from 0.1 to 2 mM with the sensitivity of 862 μA mM^{-1} cm^{-2} ($R^2 = 0.999$), the other was from 2 to 25 mM with the sensitivity of 480 μA mM^{-1} cm^{-2} ($R^2 = 0.993$). The detection limit of this electrode was calculated to be 11 μM when the signal/noise ratio was set to 3. The detection range is close to commercial glucose sensors (as a reference, Bayer Contour Plus One possesses a detection range of 0.6–33.3 mM). The recovery of the sensor in human blood serum was measured. For each sample, 90 μL serum was added into 9 mL of 0.4 M NaOH. As a result, the recoveries of 1 mM glucose in three samples were 96.6–98.5%. Performance parameters of nonenzymatic glucose sensors based on different kinds of Cu/LCM composites are compared in Table 2. Obviously, Cu/rGO-BP performed a wide linear range (up to 25 mM). In comparison with NiO-decorated buckypaper, which was reported by our group [9], the peak potential for glucose oxidation shifts from 0.58 to 0.4 V, denoting better electro-catalytic activity of Cu/rGO-BP. As a result, the upper limit of the sensor's linear range increases from 9 mM to 25 mM. Considering the fasting blood glucose concentrations for healthy people and diabetics are 3.9–6.1 mM and over 7 mM, respectively, the linear range of Cu/rGO-BP is suitable for daily blood glucose monitoring.

Table 2
Performance parameters of Cu/LCM-based glucose sensors.

Electrode	Linear range (mM)	Sensitivity (μA mM^{-1} cm^{-2})	Detection limit (μM)	Reference
Cu-MOF[a]/MWCNT/GCE[a]	5×10^{-4}–2.34, 2.34–11.84	3878, 1391	0.4	[18]
CuO/carbon cloth	0.05–3.3	785.2	0.22	[19]
Cu(II)/polyaniline/rGO/FR4	2.8–22.2 μM, Up to 4	4168.37, 525.4	4.93	[33]
Cu_2O/rGO/GCE	0.02–0.2, 0.2–1	525, 198	4.7	[34]
CuO/MWCNT/graphite	4×10^{-3}–5, 5–10, 10–14.5	1221, 619, 335	4	[35]
CuO/SWCNT/ITO[a]	5×10^{-5}–1.8	1610	0.05	[36]
CuO/rGO/GCE	2×10^{-3}–4	1360	0.7	[37]
Cu/rGO/GCE	0.05–4.5	N/A	0.5	[30]
Cu/MWCNT/GCE	Up to 7.5	1096	1	[38]
Cu/rGO-BP	0.1–2, 2–25	862, 480	11	This work

[a] Abbreviations: GCE, glassy carbon electrode; ITO, indium tin oxide.

To examine the influence of interfering species, the amperometric

responses to 1 mM glucose, 33 μM ascorbic acid (AA), 100 μM uric acid (UA) and 33 μM dopamine were compared. The amounts of the chemicals used in this test were based on the fact that the physiological levels of AA, UA and dopamine were less than 1/30, 1/10 and 1/30 of the glucose level, respectively [39,40]. As shown in Fig. 5d, the amperometric responses to the interfering species do not have significant influence: the response ratios of AA, UA and dopamine to 1 mM glucose are 4.1, 5.3 and 3.7%, respectively. The result indicates that the anti-interference performance of Cu/rGO-BP is competent for the detection of glucose.

As repeatability and reproducibility tests, the amperometric responses of three pieces of Cu/rGO-BP prepared under the same conditions were measured by two operators. Fig. 6 presents the responses to 1 mM glucose, the relative standard deviations of measurements by Operator 1, Operator 2 and all 6 measurements are 2.87, 2.55 and 3.02%, respectively. In order to investigate the stability of Cu/rGO-BP, it was stored in ambient environment after its first test. After 30 days the response to 1 mM glucose was measured again and the decrease was less than 2%.

The sheet resistances of SWCNT buckypaper and Cu/rGO-BP measured by 4-probe system are 20.1 and 33.2 Ω/ϒ, respectively. The result proves that SWCNT buckypaper is capable of providing excellent conductivity. Combining the structural characterizations and electrochemical measurements of Cu/rGO-BP, it can be deduced that both SWCNT and rGO play significant roles in Cu/rGO-BP. On one hand, highly crystallized SWCNT is a promising support material for biosensors due to its satisfying flexibility, chemical stability and electrical conductivity. On the other hand, rGO can serve as an ideal intermediate between SWCNT and catalyst. In other words, the designed Cu/rGO-BP as a flexible electrode has been successfully implemented through the proposed strategy in this work. Additionally, the fabrication strategy for Cu/rGO-BP is scalable, environment-friendly and low-cost. Since $Cu(OH)_2$/GO is efficiently reduced in H_2 at 500 °C, this method should be valid for the preparation of other metal/rGO composites. In summary, the fabrication strategy for Cu/rGO-BP is promising in flexible bioelectronic devices.

4. Conclusions

A novel green strategy has been designed and developed to fabricate Cu/rGO-BP as a flexible electrode for glucose detection. Taking advantage of GO and SWCNT, Cu/rGO-BP electrode exhibited outstanding flexibility and electro-catalytic activity. Glucose was oxidized at a low potential (0.4 V) on this electrode and the glucose sensor based on Cu/rGO-BP manifested a high upper limit of linear range (25 mM) with a sensitivity of 480 μA mM^{-1} cm^{-2}. Considering the interaction between different metal oxides and H_2 at high temperature, this fabrication strategy for Cu/rGO-BP can also be applied to flexible buckypaper electrodes modified with other metals or metal oxides (Ag, Pd, Pt, Au, Al_2O_3, TiO_2, MnO_2, ZnO, etc.) for electrochemical applications.

CRediT authorship contribution statement

Tianxiang Zhu: Conceptualization, Investigation, Methodology, Visualization, Writing-Original Draft, Writing-review & editing.

Xiaoer Wang, Weiwei Chang: Investigation, Methodology.

Yifan Zhang: Visualization.

Takahiro Maruyama: Supervision, Resources.

Liqiang Luo, Xinluo Zhao: Conceptualization, Methodology, Supervision, Resources, Funding acquisition, Writing-Original Draft, Writing-review & editing.

Declaration of competing interest

The authors declare that they have no known competing financial interests or personal relationships that could have appeared to influence the work reported in this paper.

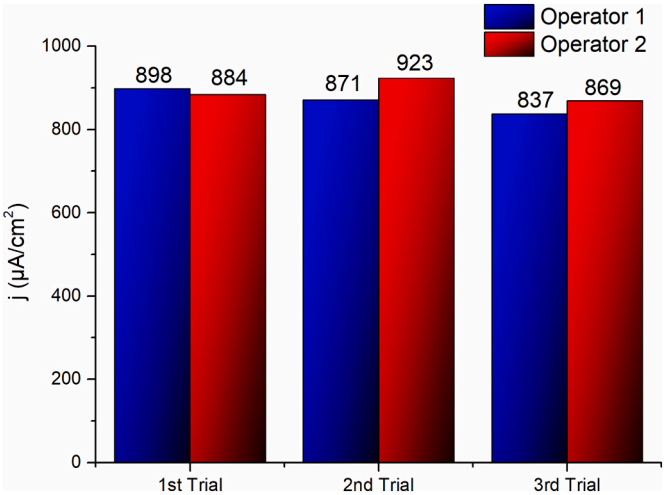

Fig. 6. Results of repeatability and reproducibility tests.

Acknowledgements

This work is supported by the National Natural Science Foundation of China (grant Nos.: 61571278, 61971274).

Appendix A. Supplementary data

Supplementary data to this article can be found online at https://doi.org/10.1016/j.msec.2020.111757.

References

[1] S. Kumar, R. Rani, N. Dilbaghi, K. Tankeshwar, K.H. Kim, Carbon nanotubes: a novel material for multifaceted applications in human healthcare, Chem. Soc. Rev. 46 (2017) 158–196, https://doi.org/10.1039/C6CS00517A.

[2] V.R. Raphey, T.K. Henna, K.P. Nivitha, P. Mufeedha, C. Sabu, K. Pramod, Advanced biomedical applications of carbon nanotube, Mater. Sci. Eng., C 100 (2019) 616–630, https://doi.org/10.1016/j.msec.2019.03.043.

[3] M.F.L. De Volder, S.H. Tawfick, R.H. Baughman, A.J. Hart, Carbon nanotubes: present and future commercial applications, Science 339 (2013) 535–539, https://doi.org/10.1126/science.1222453.

[4] X. Chen, L. Yin, J. Lv, A.J. Gross, M. Le, N.G. Gutierrez, Y. Li, I. Jeerapan, F. Giroud, A. Berezovska, R.K. O'Reilly, S. Xu, S. Cosnier, J. Wang, Stretchable and flexible buckypaper-based lactate biofuel cell for wearable electronics, Adv. Funct. Mater. 29 (2019) 1905785, https://doi.org/10.1002/adfm.201905785.

[5] G. Yang, L. Liu, Z. Wu, Improved strain sensing capability of nano-carbon free-standing buckypapers based strain gauges, Smart Mater. Struct. 28 (2019), 065009, https://doi.org/10.1088/1361-665X/ab147e.

[6] X. Wang, H. Wei, X. Liu, W. Du, X. Zhao, X. Wang, Novel three-dimensional polyaniline nanothorns vertically grown on buckypaper as high-performance supercapacitor electrode, Nanotechnology 30 (2019) 325401, https://doi.org/10.1088/1361-6528/ab156d.

[7] T. Leng, H.A. Fishman, Carbon nanotube bucky paper as an artificial support membrane for retinal cell transplantation, Ophthalmic Surg. Laser. Imag. 44 (2013) 73–76, https://doi.org/10.3928/23258160-20121221-16.

[8] Y. Su, Y. Zhang, Carbon nanomaterials synthesized by arc discharge hot plasma, Carbon 83 (2015) 90–99, https://doi.org/10.1016/j.carbon.2014.11.023.

[9] T. Zhu, Y. Zhang, L. Luo, X. Zhao, Facile fabrication of NiO-decorated double-layer single-walled carbon nanotube buckypaper for glucose detection, ACS Appl. Mater. Interfaces 11 (2019) 10856–10861, https://doi.org/10.1021/acsami.9b00803.

[10] S. Pei, H.M. Cheng, The reduction of graphene oxide, Carbon 50 (2012) 3210–3228, https://doi.org/10.1016/j.carbon.2011.11.010.

[11] A.S. Dezfuli, M.R. Ganjali, H.R. Naderi, Anchoring samarium oxide nanoparticles on reduced graphene oxide for high-performance supercapacitor, Appl. Surf. Sci. 402 (2017) 245–253, https://doi.org/10.1016/j.apsusc.2017.01.021.

[12] R. Atchudan, T.N.J.I. Edison, S. Perumal, D. Karthikeyan, Y.R. Lee, Facile synthesis of zinc oxide nanoparticles decorated graphene oxide composite via simple solvothermal route and their photocatalytic activity on methylene blue degradation, J. Photochem. Photobiol. B-Biol. 162 (2016) 500–510, https://doi.org/10.1016/j.jphotobiol.2016.07.019.

[13] K. Wu, X. Liu, Z. Li, Y. Jiao, C. Zhou, Fabrication of chitosan/graphene oxide composite aerogel microspheres with high bilirubin removal performance, Mater. Sci. Eng., C 106 (2020) 110162, https://doi.org/10.1016/j.msec.2019.110162.

[14] L. Chen, D.J. Magliano, P.Z. Zimmet, The worldwide epidemiology of type 2 diabetes mellitus – present and future perspectives, Nat. Rev. Endocrinol. 8 (2011) 228–236, https://doi.org/10.1038/nrendo.2011.183.
[15] J. Ye, D. Deng, Y. Wang, L. Luo, K. Qian, S. Cao, X. Feng, Well-aligned Cu@C nanocubes for highly efficient nonenzymatic glucose detection in human serum, Sens. Actuator B-Chem. 305 (2020) 127473, https://doi.org/10.1016/j.snb.2019.127473.
[16] L. Tang, K. Huan, D. Deng, L. Han, Z. Zeng, L. Luo, Glucose sensor based on Pd nanosheets deposited on Cu/Cu_2O nanocomposites by galvanic replacement, Colloid Surf. B-Biointerfaces 188 (2020) 110797, https://doi.org/10.1016/j.colsurfb.2020.110797.
[17] N. Yang, K. Guo, Y. Zhang, C. Xu, Engineering the valence state of ZIF-67 by Cu_2O for efficient nonenzymatic glucose detection, J. Mater. Chem. B 8 (2020) 2856–2861, https://doi.org/10.1039/d0tb00094a.
[18] L. Wu, Z. Lu, J. Ye, Enzyme-free glucose sensor based on layer-by-layer electrodeposition of multilayer films of multi-walled carbon nanotubes and Cu-based metal framework modified glassy carbon electrode, Biosens. Bioelectron. 135 (2019) 45–49, https://doi.org/10.1016/j.bios.2019.03.064.
[19] S. Sun, N. Shi, B. Zhang, X. Liao, Z. Huang, X. Chen, X. Pu, G. Yin, Hierarchically porous CuO spindle-like nanosheets grown on a carbon cloth for sensitive non-enzymatic glucose sensor, Nanotechnology 31 (2020) 375502, https://doi.org/10.1088/1361-6528/ab96e2.
[20] X. Zhao, S. Inoue, M. Jinno, T. Suzuki, Y. Ando, Macroscopic oriented web of single-wall carbon nanotubes, Chem. Phys. Lett. 373 (2003) 266–271, https://doi.org/10.1016/S0009-2614(03)00610-9.
[21] L. Sheng, L. Shi, K. An, L. Yu, Y. Ando, X. Zhao, Effective and efficient purification of single-wall carbon nanotubes based on hydrogen treatment, Chem. Phys. Lett. 502 (2011) 101–106, https://doi.org/10.1016/j.cplett.2010.12.034.
[22] J. Wei, Z. Zang, Y. Zhang, M. Wang, J. Du, X. Tang, Enhanced performance of light-controlled conductive switching in hybrid cuprous oxide/reduced graphene oxide (Cu_2O/rGO) nanocomposites, Opt. Lett. 42 (2017) 911–914, https://doi.org/10.1364/OL.42.000911.
[23] K. Krishnamoorthy, M. Veerapandian, K. Yun, S.J. Kim, The chemical and structural analysis of graphene oxide with different degrees of oxidation, Carbon 53 (2013) 38–49, https://doi.org/10.1016/j.carbon.2012.10.013.
[24] M.S. Dresselhaus, G. Dresselhaus, R. Saito, A. Jorio, Raman spectroscopy of carbon nanotubes, Phys. Rep. 409 (2005) 47–99, https://doi.org/10.1016/j.physrep.2004.10.006.
[25] H. Kuzmany, W. Plank, M. Hulman, C. Kramberger, A. Grüneis, T. Pichler, H. Peterlik, H. Kataura, Y. Achiba, Determination of SWCNT diameters from the Raman response of the radial breathing mode, Eur. Phys. J. B 22 (2001) 307–320, https://doi.org/10.1007/s100510170108.
[26] W. Gao, L.B. Alemany, L. Ci, P.M. Ajayan, New insights into the structure and reduction of graphite oxide, Nat. Chem. 1 (2009) 403–408, https://doi.org/10.1038/NCHEM.281.
[27] V.C. Tung, M.J. Allen, Y. Yang, R.B. Kaner, High-throughput solution processing of large-scale graphene, Nat. Nano. 4 (2009) 25–29, https://doi.org/10.1038/NNANO.2008.329.
[28] T.V. Cuong, V.H. Pham, Q.T. Tran, S.H. Hahn, J.S. Chung, E.W. Shin, E.J. Kim, Photoluminescence and Raman studies of graphene thin films prepared by reduction of graphene oxide, Mater. Lett. 64 (2010) 399–401, https://doi.org/10.1016/j.matlet.2009.11.029.
[29] J. Wang, X. Sun, X. Cai, Y. Lei, L. Song, S. Xie, Nonenzymatic glucose sensor using freestanding single-wall carbon nanotube films, Electrochem. Solid State Lett. 10 (2007) J58–J60, https://doi.org/10.1149/1.2710184.
[30] J. Luo, S. Jiang, H. Zhang, J. Jiang, X. Liu, A novel non-enzymatic glucose sensor based on Cu nanoparticle modified graphene sheets electrode, Anal. Chim. Acta 709 (2012) 47–53, https://doi.org/10.1016/j.aca.2011.10.025.
[31] S.T. Farrell, C.B. Breslin, Oxidation and photo-induced oxidation of glucose at a polyaniline film modified by copper particles, Electrochim. Acta 49 (2004) 4497–4503, https://doi.org/10.1016/j.electacta.2004.05.007.
[32] J.M. Marioli, T. Kuwana, Electrochemical characterization of carbohydrate oxidation at copper electrodes, Electrochim. Acta 37 (1992) 1187–1197, https://doi.org/10.1016/0013-4686(92)85055-P.
[33] V.K. Anand, A. Bukke, K. Bhatt, S. Kumar, S. Sharma, R. Goyal, G.S. Virdi, Highly sensitive and reusable Cu^{+2}/polyaniline/reduced graphene oxide nanocomposite ink-based non-enzymatic glucose sensor, Appl. Phys. A-Mater. Sci. Process. 126 (2020) 1–11, https://doi.org/10.1007/s00339-020-03620-4.
[34] H. Xie, Q. Ke, X. Xiong, Preparation of a Cu_2O/rGO porous composite through a double-sacrificial-template method for non-enzymatic glucose detection, J. Mater. Sci. 52 (2017) 5652–5660, https://doi.org/10.1007/s10853-017-0800-8.
[35] X.W. Liu, P. Pan, Z.M. Zhang, F. Guo, Z.C. Yang, J. Wei, Z. Wei, Ordered self-assembly of screen-printed flower-like CuO and CuO/MWCNTs modified graphite electrodes and applications in non-enzymatic glucose sensor, J. Electroanal. Chem. 763 (2016) 37–44, https://doi.org/10.1016/j.jelechem.2015.12.039.
[36] N.Q. Dung, D. Patil, H. Jung, D. Kim, A high-performance nonenzymatic glucose sensor made of CuO-SWCNT nanocomposites, Biosens. Bioelectron. 42 (2013) 280–286, https://doi.org/10.1016/j.bios.2012.10.044.
[37] L. Luo, L. Zhu, Z. Wang, Nonenzymatic amperometric determination of glucose by CuO nanocubes-graphene nanocomposite modified electrode, Bioelectrochemistry 88 (2012) 156–163, https://doi.org/10.1016/j.bioelechem.2012.03.006.
[38] J. Yang, W.D. Zhang, S. Gunasekaran, An amperometric non-enzymatic glucose sensor by electrodepositing copper nanocubes onto vertically well-aligned multi-walled carbon nanotube arrays, Biosens. Bioelectron. 26 (2010) 279–284, https://doi.org/10.1016/j.bios.2010.06.014.
[39] P.P. Tomanin, P.V. Cherepanov, Q.A. Besford, A.J. Christofferson, A. Amodio, C. F. McConville, I. Yarovsky, F. Caruso, F. Cavalieri, Cobalt phosphate nanostructures for non-enzymatic glucose sensing at physiological pH, ACS Appl. Mater. Interfaces 10 (2018) 42786–42795, https://doi.org/10.1021/acsami.8b12966.
[40] Z. Ren, H. Mao, H. Luo, Y. Liu, Glucose sensor based on porous Ni by using a graphene bottom layer combined with a Ni middle layer, Carbon 149 (2019) 609–617, https://doi.org/10.1016/j.carbon.2019.04.073.